Supporting information

for

1,2-Migration of *N*-Diarylboryl Imidazol-2-ylidene through Intermolecular Radical Process

Wei-Chun Liu, Yi-Hung Liu, Tien-Sung Lin, Shie-Ming Peng, Ching-Wen Chiu*

Department of Chemistry, National Taiwan University, No. 1, Section 4, Roosevelt Road, Taipei 10617, Taiwan

1. Structural determination.

(1) Crystal data of [1-Aa][OTf]

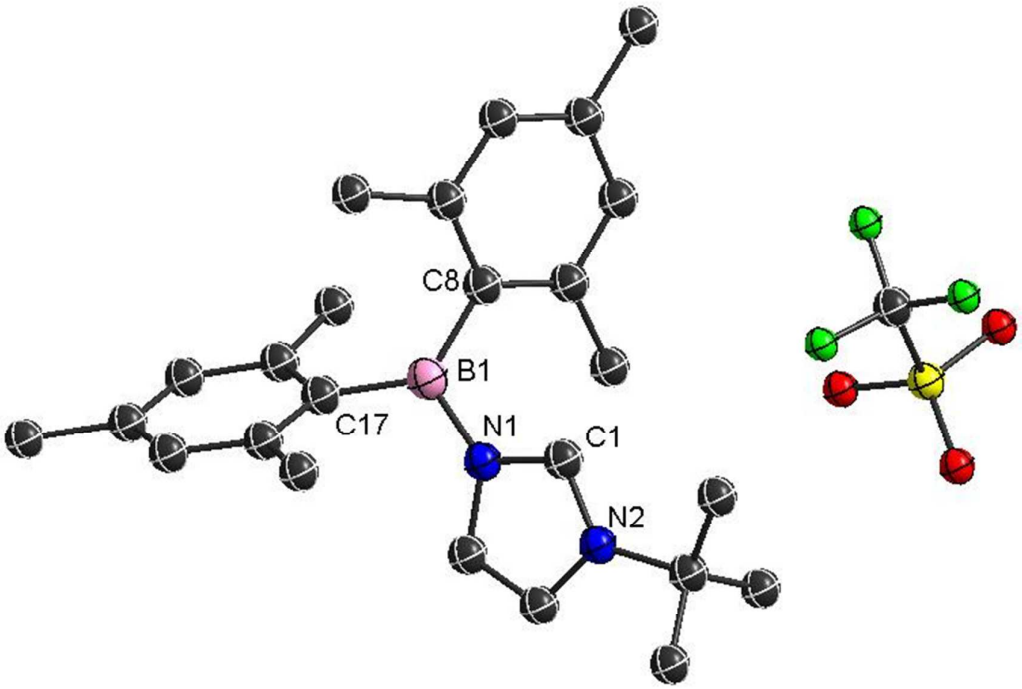

Figure S1: Crystal structure of [**1-Aa**][OTf]

Selected bond distances (Å) and angles (deg): N(1)–C(1) 1.347(5), N(1)-B(1) 1.494(5), N(2)-C(1) 1.324(4), B(1)-C(8) 1.555(5),B(1)-C(17) 1.560(5) N(1)-B(1)-C(8)116.3(3), N(1)-B(1)-C(17)116.6(3), C(8)-B(1)-C(17)127.1(3), N(2)-C(1)-N(1)110.0(3), C(1)-N(1)-B(1)126.0(3)

Table S1. Crystal data and experimental details for [1-Aa][OTf].

Crystal data		
Empirical formula	C29 H37 B F3 N2 O3 S	
Formula weight	561.47	
Crystal system	Monoclinic	
Space group	C2/c	
Unit cell dimensions	a = 34.9981(12) Å	α= 90°.
	b = 8.6337(5) Å	β= 99.807(4)°.
	c = 19.3753(9) Å	γ = 90°.
Volume	5768.9(5) $Å^3$	
Z	8	
F(000)	2376	
Density (calculated)	1.293 Mg/m^3	
Wavelength	1.54178 Å	
Cell parameters reflections used	2723	
Theta range for Cell parameters	4.6010 to 74.8830°.	
Absorption coefficient	1.441 mm^{-1}	
Temperature	150(2) K	
Crystal size	0.35 x 0.20 x 0.10 mm^3	
Data collection		
Diffractometer	Xcalibur, Atlas, Gemini	
Absorption correction	Semi-empirical from equivalents	
Max. and min. transmission	1.00000 and 0.88669	
No. of measured reflections	10437	
No. of independent reflections	5223 [R(int) = 0.0444]	
No. of observed [I>2_igma(I)]	3539	
Completeness to theta = 67.679°	99.3 %	
Theta range for data collection	4.632 to 67.995°.	
Refinement		
Final R indices [I>2sigma(I)]	R1 = 0.0691, wR2 = 0.1781	
R indices (all data)	R1 = 0.1036, wR2 = 0.2074	
Goodness-of-fit on F^2	1.083	
No. of reflections	5223	
No. of parameters	353	
No. of restraints	37	
Largest diff. peak and hole	0.807 and -0.821 e.$Å^{-3}$	

(2) Crystal data of 3-Aa

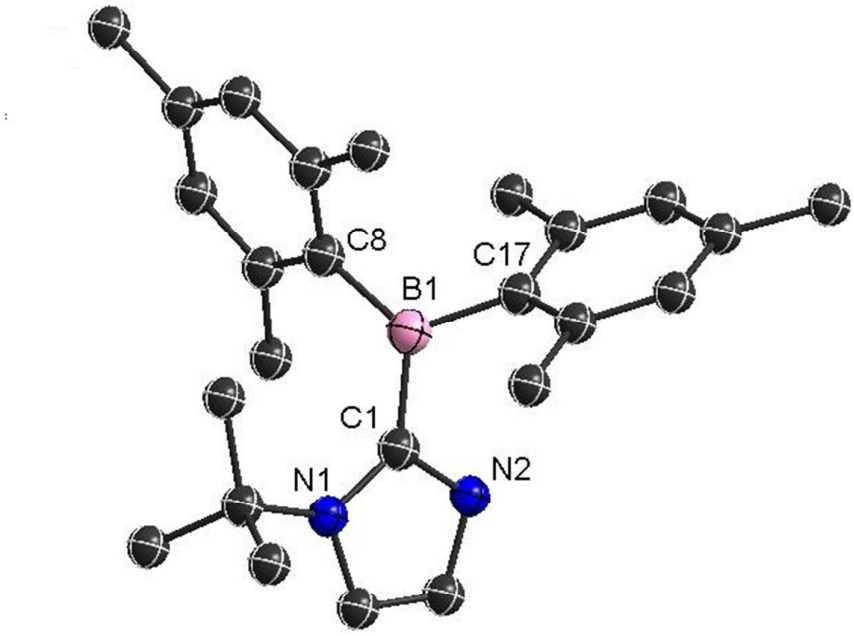

Figure S2: Crystal structure of **3-Aa**.

Selected bond distances (Å) and angles (deg): N(1)-C(1) 1.376(3), N(2)-C(1) 1.339(3), B(1)-C(1) 1.574(3), B(1)-C(8) 1.576(3), B(1)-C(17) 1.571(3), C(8)-B(1)-C(17) 119.7(2), C(8)-B(1)-C(1) 125.5(2), C(17)-B(1)-C(1) 114.30(19), N(2)-C(1)-B(1) 114.3(2), N(1)-C(1)-B(1) 135.1(2)

Table S2. Crystal data and structure refinement for 3-Aa

Crystal data		
Empirical formula	C25 H33 B N2	
Formula weight	372.34	
Crystal system	Orthorhombic	
Space group	Pbca	
Unit cell dimensions	a = 9.86510(10) Å	α= 90°.
	b = 15.8816(2) Å	β= 90°.
	c = 28.1381(4) Å	γ = 90°.
Volume	4408.50(9) $Å^3$	
Z	8	
F(000)	1616	
Density (calculated)	1.122 Mg/m^3	
Wavelength	1.54178 Å	
Cell parameters reflections used	4413	
Theta range for Cell parameters	3.1340 to 74.5470°.	
Absorption coefficient	0.482 mm^{-1}	
Temperature	150(2) K	
Crystal size	0.35 x 0.30 x 0.25 mm^3	
Data collection		
Diffractometer	Xcalibur, Atlas, Gemini	
Absorption correction	Semi-empirical from equivalents	
Max. and min. transmission	1.00000 and 0.87800	
No. of measured reflections	10076	
No. of independent reflections	4009 [R(int) = 0.0275]	
No. of observed [I>2_igma(I)]	3204	
Completeness to theta = 67.679°	99.9 %	
Theta range for data collection	3.141 to 67.987°.	
Refinement		
Final R indices [I>2sigma(I)]	R1 = 0.0765, wR2 = 0.2133	
R indices (all data)	R1 = 0.0902, wR2 = 0.2284	
Goodness-of-fit on F^2	1.421	
No. of reflections	4009	
No. of parameters	253	
No. of restraints	0	
Largest diff. peak and hole	0.511 and -0.496 e.$Å^{-3}$	

(3) Crystal data of $(3\text{-Bb})_2$

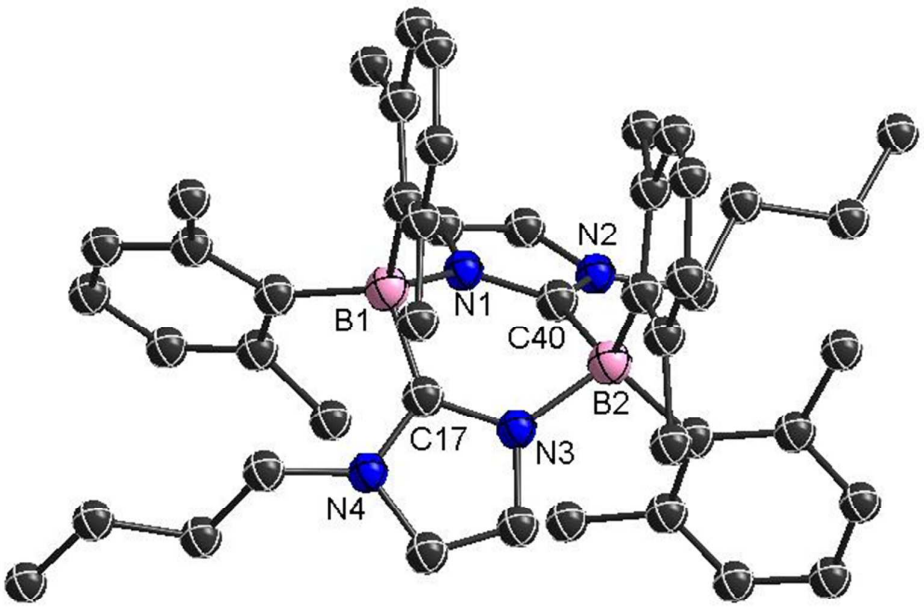

Figure S3: Crystal structure of $(\mathbf{3\text{-}Bb})_2$

Selected bond distances (Å) and angles (deg): N(1)-C(40) 1.348(4), N(1)-B(1) 1.633(4), N(2)-C(40) 1.357(4), N(3)-C(17) 1.351(4), N(4)-C(17) 1.355(4), B(1)-C(17) 1.635(4), B(1)-C(9) 1.665(4), B(1)-C(1) 1.664(4), B(2)-C(40) 1.641(4), B(2)-C(32) 1.658(4), B(2)-C(24) 1.659(4), C(40)-N(1)-B(1) 125.0(2), C(17)-N(3)-B(2) 124.6(2), N(1)-B(1)-C(17) 99.7(2), N(3)-B(2)-C(40) 99.3(2), N(3)-C(17)-N(4)107.0(2), N(3)-C(17)-B(1) 124.6(2), N(4)-C(17)-B(1) 128.2(2), N(1)-C(40)-N(2) 107.3(2), N(1)-C(40)-B(2) 124.2(2), N(2)-C(40)-B(2) 128.4(2)

Table S3. Crystal data and experimental details for $(3\text{-Bb})_2$.

Crystal data		
Empirical formula	C46 H58 B2 N4	
Formula weight	688.58	
Crystal system	Monoclinic	
Space group	$P2_1/c$	
Unit cell dimensions	a = 18.8404(4) Å	α= 90°.
	b = 25.3026(4) Å	β= 119.635(3)°.
	c = 18.8088(5) Å	γ = 90°.
Volume	7793.5(4) $Å^3$	
Z	8	
F(000)	2976	
Density (calculated)	1.174 Mg/m^3	
Wavelength	0.71073 Å	
Cell parameters reflections used	23870	
Theta range for Cell parameters	3.2930 to 28.6040°.	
Absorption coefficient	0.067 mm^{-1}	
Temperature	150(2) K	
Crystal size	0.20 x 0.15 x 0.10 mm^3	
Data collection		
Diffractometer	Xcalibur, Atlas, Gemini	
Absorption correction	Semi-empirical from equivalents	
Max. and min. transmission	1.00000 and 0.98883	
No. of measured reflections	114769	
No. of independent reflections	13715 [R(int) = 0.0581]	
No. of observed [I>2_igma(I)]	9865	
Completeness to theta = 25.000°	99.8 %	
Theta range for data collection	2.716 to 25.000°.	
Refinement		
Final R indices [I>2sigma(I)]	R1 = 0.0821, wR2 = 0.2213	
R indices (all data)	R1 = 0.1112, wR2 = 0.2430	
Goodness-of-fit on F^2	1.200	
No. of reflections	13715	
No. of parameters	966	
No. of restraints	235	
Largest diff. peak and hole	0.933 and -0.547 e.$Å^{-3}$	

2. NMR spectra of crossover experiments

(1) [1-Aa][OTf]+[1-Bb][OTf]+LiHMDS

A solution of [**1-Aa**][OTf] (50 mg, 0.093 mmol) and [**1-Bb**][OTf] (50 mg, 0.098 mmol) dissolved in C_6D_6 were added to LiHMDS (31.9 mg, 0.191 mmol). After addition, color changed from colorless to blue-green. The NMR spectrum was recorded without further purification.

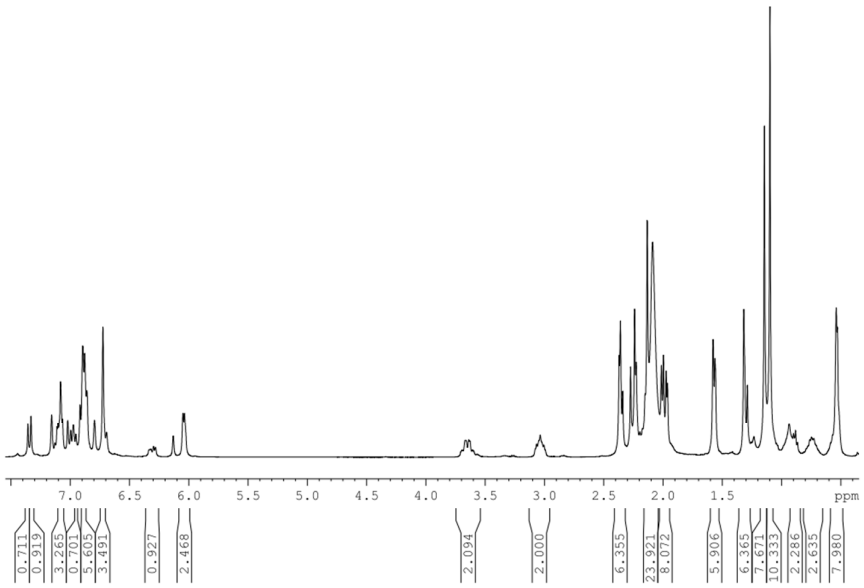

Figure S4: ^{1}H NMR of crude mixtures in C_6D_6

(2) (3-Bb)$_2$ + (3-Ba)$_2$ + (3-Bb/3-Ba)

In 4 ml vials, freshly synthesized (**3-Ba**) and (**3-Bb**) were mixed in C_6D_6 and transferred into a Young's NMR tube. NMR spectrum was recorded after one day of the completeness of the dimerization.

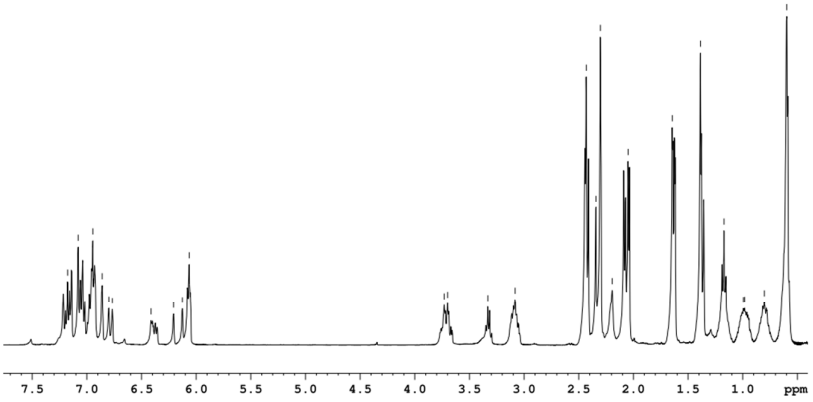

Figure S5: ^{1}H NMR of (**3-Ba**)$_2$, (**3-Bb**)$_2$ and (**3-Ba**/**3-Bb**) in C_6D_6

(3) Comparison of spectra

Compared the spectrums of independently generated migration compounds with the crude spectrum, signals of the crossover and non-crossover products can be identified, confirming the intermolecular migration process.

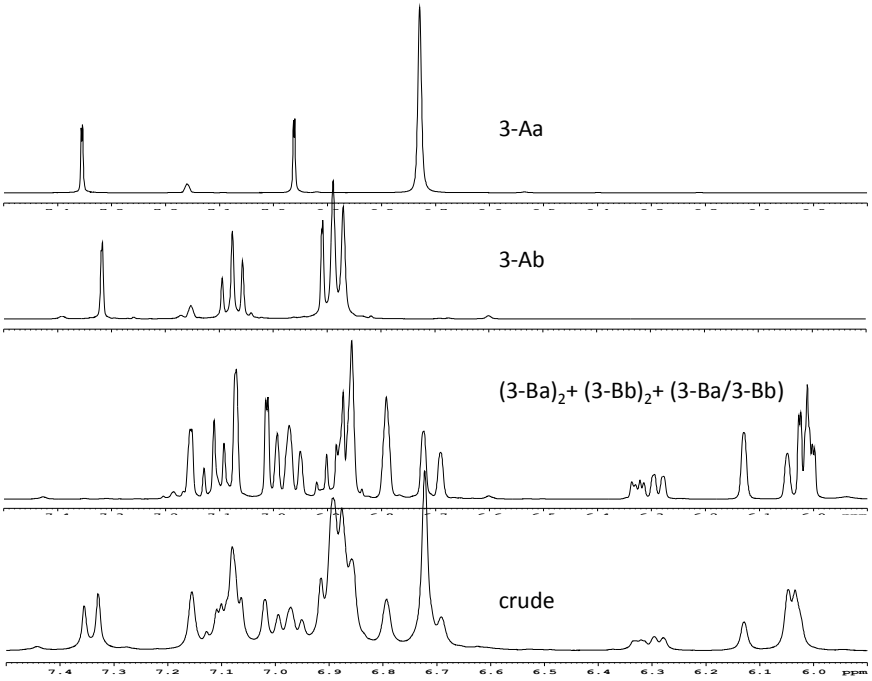

Figure S6: Aromatic region of spectra in C_6D_6

3. EPR spectra of radical trapping experiments

(1) Deprotonation with LiHMDS in the presence of DMPO

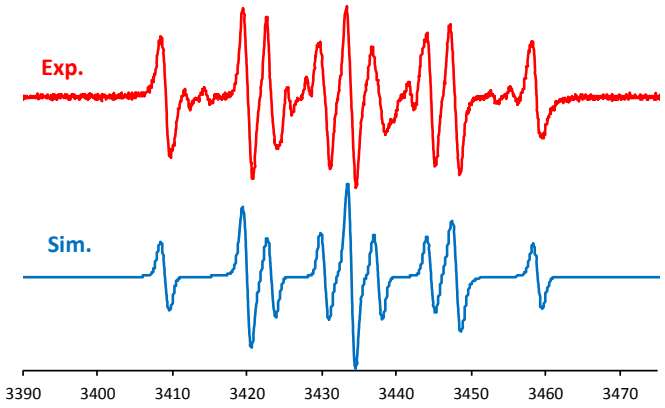

Figure S7: EPR spectrum of the DMPO trapping experiment (top) and simulated spectrum (bottom).

Table S4: Parameters used in spectral simulation

	Sys 1 (radical **4**)	Sys 2 (radical **5**)
g	[2.0035,2.0025,2.0015]	[2.0035,2.0025,2.0015]
Lw (Lorentzian, in mT)	0.13	0.11
Nucs	^{14}N, ^{1}H	^{14}N
A (in MHz)	[15,15,90;25,25,130]	[15,15,88]
Weight	2.5	3
Logtcorr*	- 10.5	- 9.6

*Note: Correlation time: logtcorr=-10.5 (=log $10^{-10.5}$ sec)

(2) Deprotonation with NaHMDS or KHMDS in the presence of DMPO

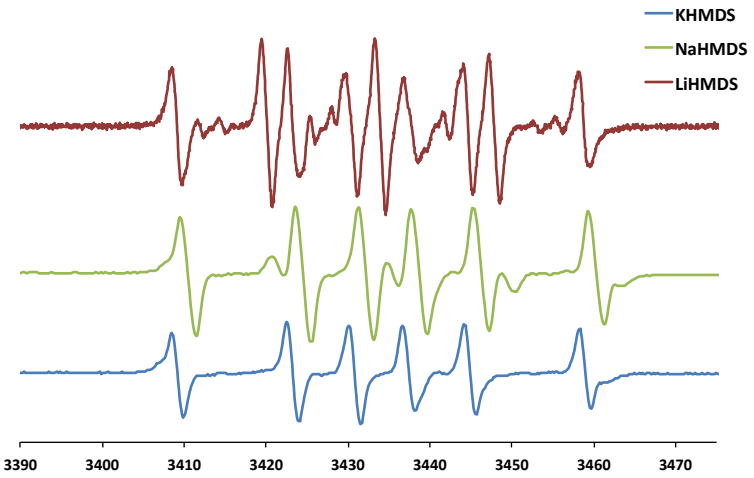

Figure S8: EPR spectra of [**1-Aa**][OTf] treated with different bases in the presence of DMPO.

(3) Independent generation of DMPO-boryl radical

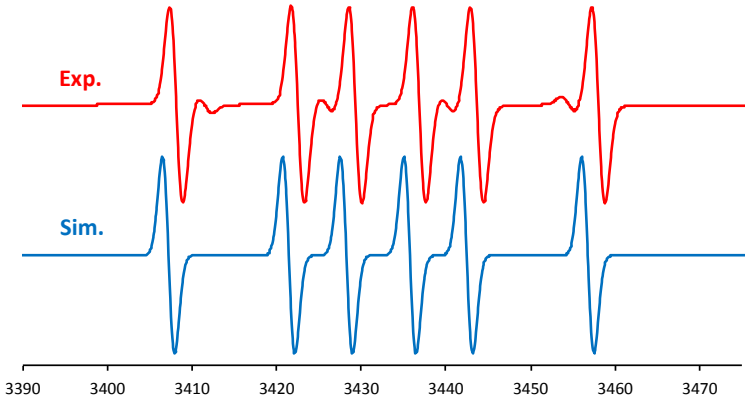

Figure S9: EPR spectrum of the DMPO-boryl radical (top) and simulated spectrum (bottom).

Table S5: Parameters used in spectral simulation

	Sys 1 (radical **4**)
g	[2.0037]
Lw (Lorentzian, in mT)	0.17
Nucs	^{14}N, ^{1}H
A (in MHz)	[40,59]
Opt. Method	perturb
Opt. nKnots	[61 0]

(4) Independent generation of aminyl radical

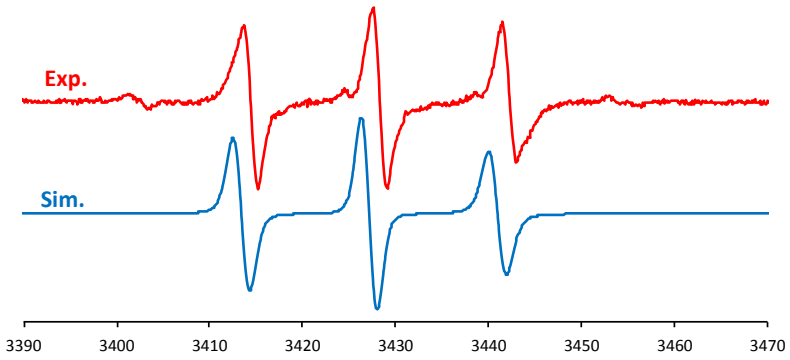

Figure S10: EPR spectrum of the aminyl radical (top) and simulated spectrum (bottom).

Table S6: Parameters used in spectral simulation

	Sys 1 (radical **5**)
g	[2.0075,2.0065,2.0055]
Lw (Lorentzian, in mT)	0.18
Nucs	^{14}N
A (in MHz)	[16,16,84]
Logtcorr	- 9.4

4. NMR Spectra

(1) [1-Aa][OTf]

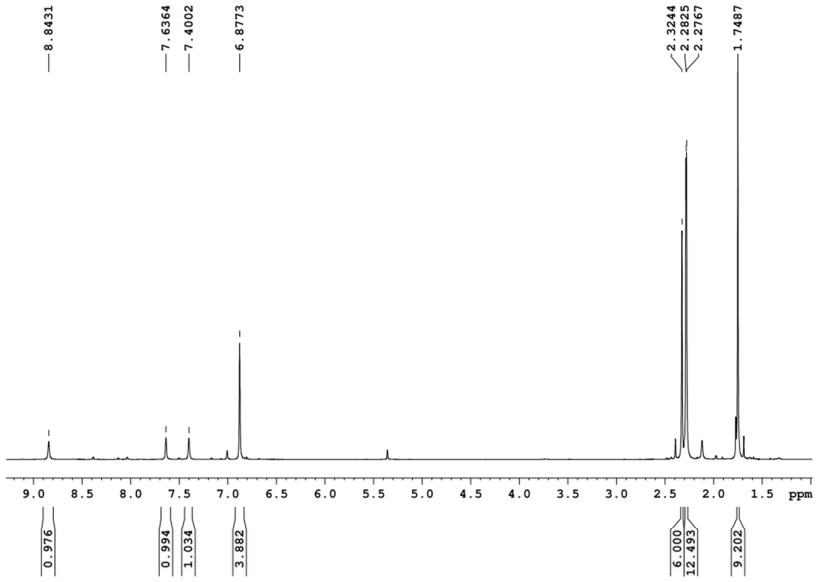

Figure S11: ^{1}H NMR of [**1-Aa**][OTf] in CD_2Cl_2

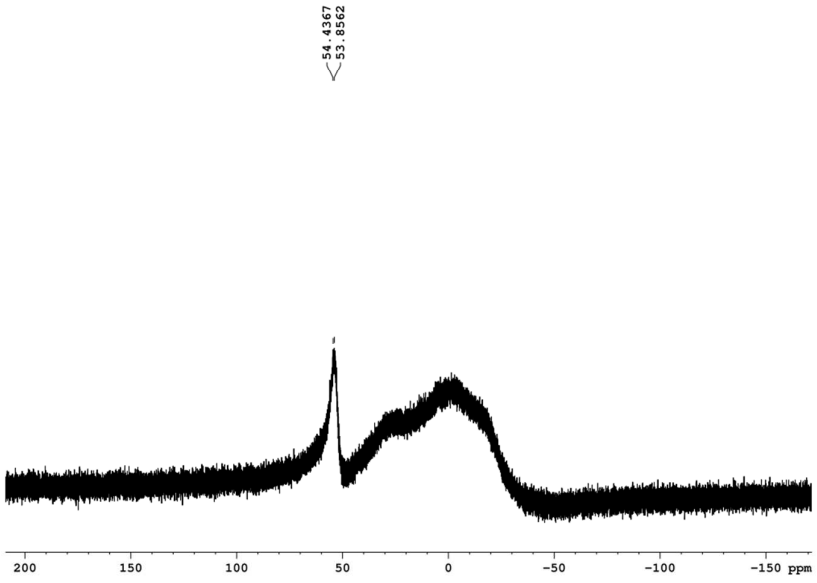

Figure S12: ^{11}B NMR of [**1-Aa**][OTf] in CD_2Cl_2

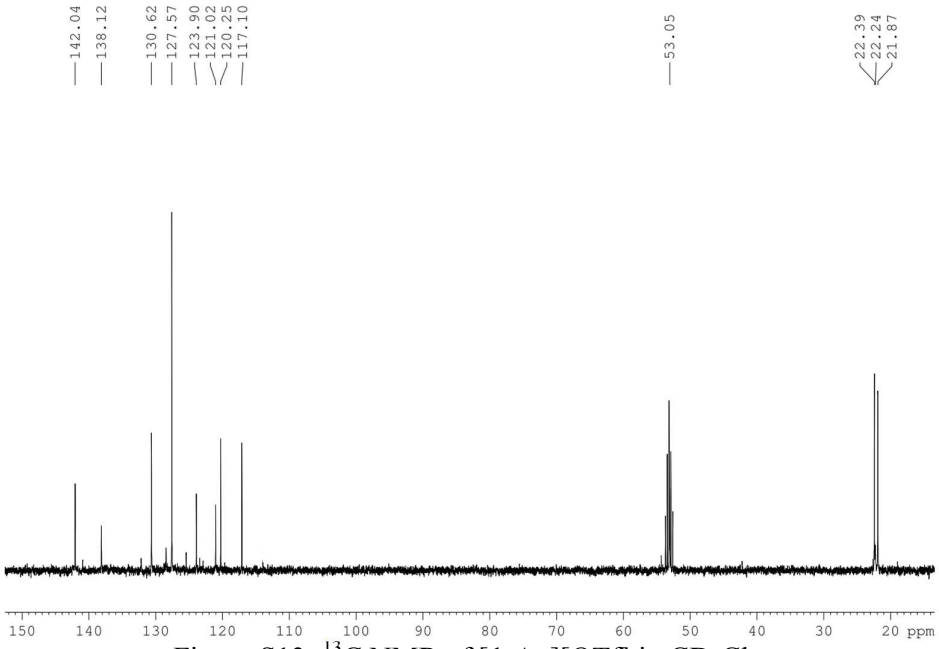

Figure S13: ^{13}C NMR of [**1-Aa**][OTf] in CD_2Cl_2

(2) [1-Bb][OTf]

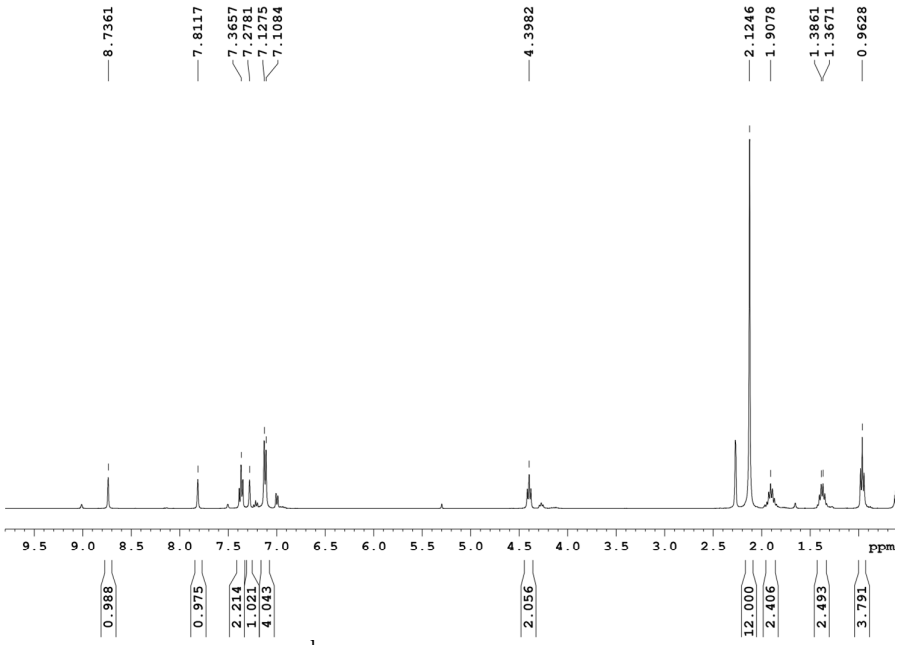

Figure S14: ^{1}H NMR of [**1-Bb**][OTf] in CD_2Cl_2

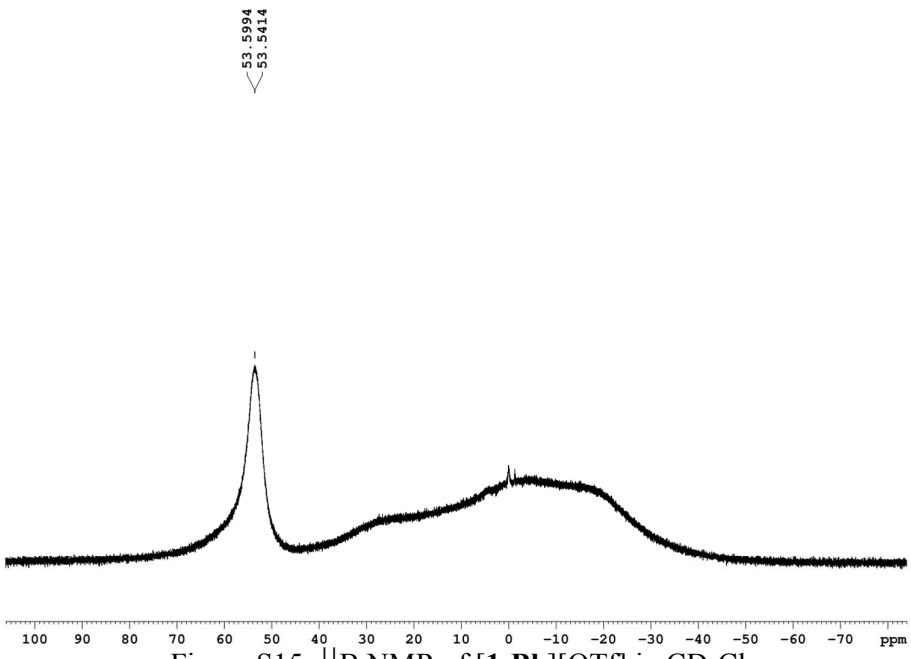

Figure S15: ^{11}B NMR of [**1-Bb**][OTf] in CD_2Cl_2

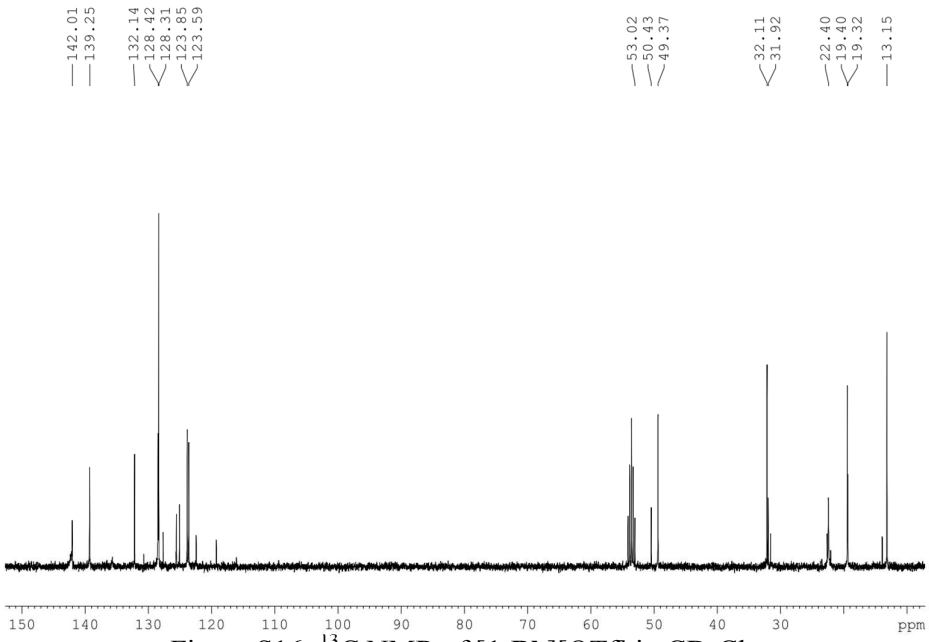

Figure S16: ^{13}C NMR of [**1-Bb**][OTf] in CD_2Cl_2

(3) [1-Ab][OTf]

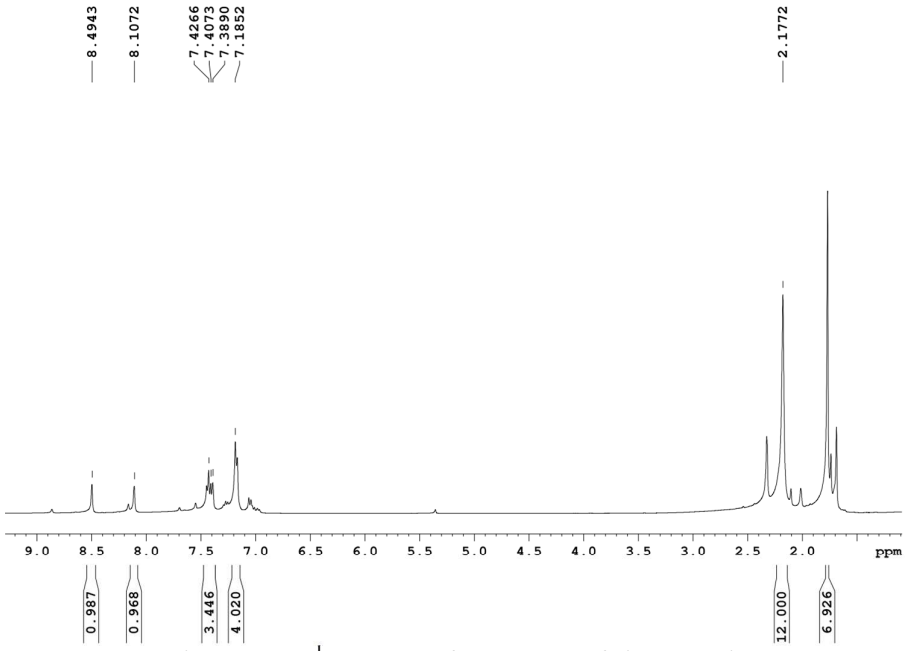

Figure S17: ^{1}H NMR of [**1-Ab**][OTf] in CD_2Cl_2

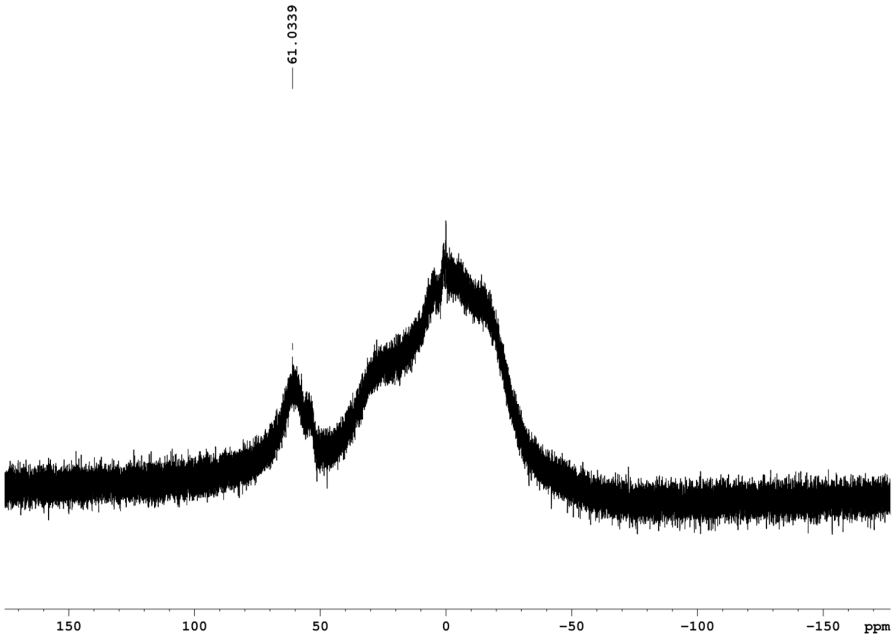

Figure S18: ^{11}B NMR of [**1-Ab**][OTf] in CD_2Cl_2

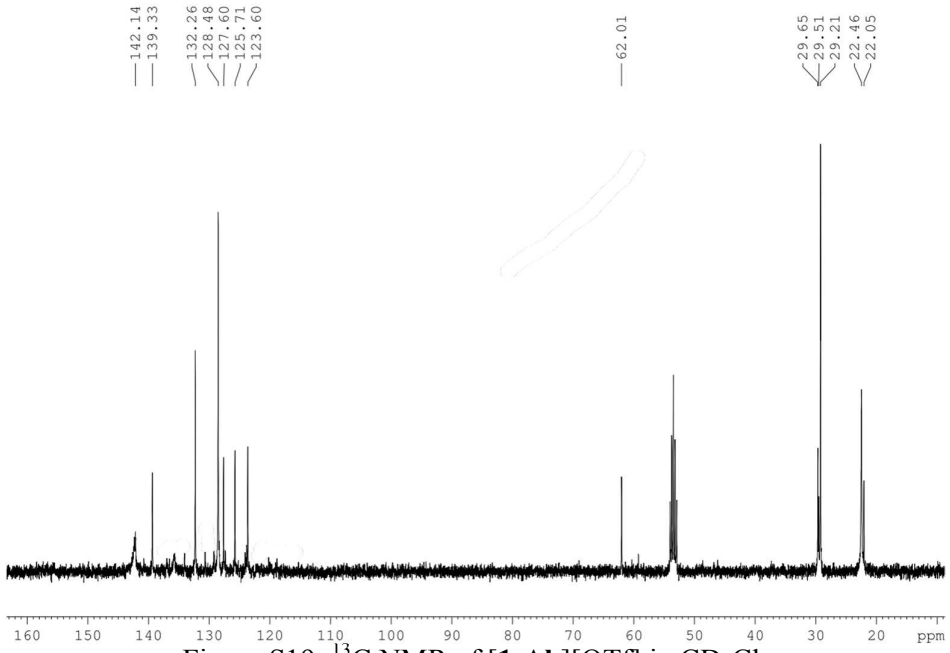

Figure S19: ^{13}C NMR of [**1-Ab**][OTf] in CD_2Cl_2

(4) [1-Ba][OTf]

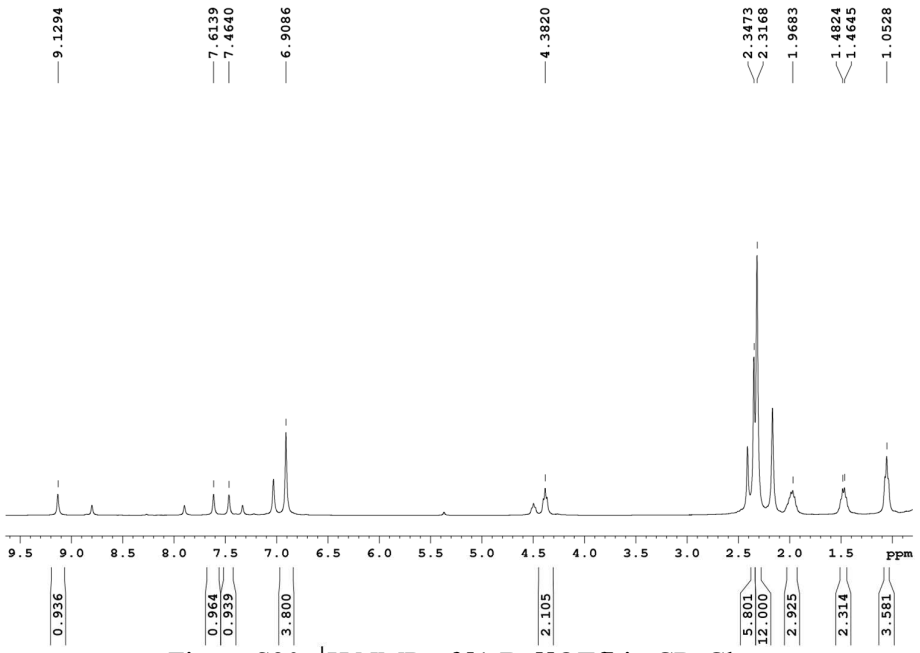

Figure S20: ^{1}H NMR of [**1-Ba**][OTf] in CD_2Cl_2

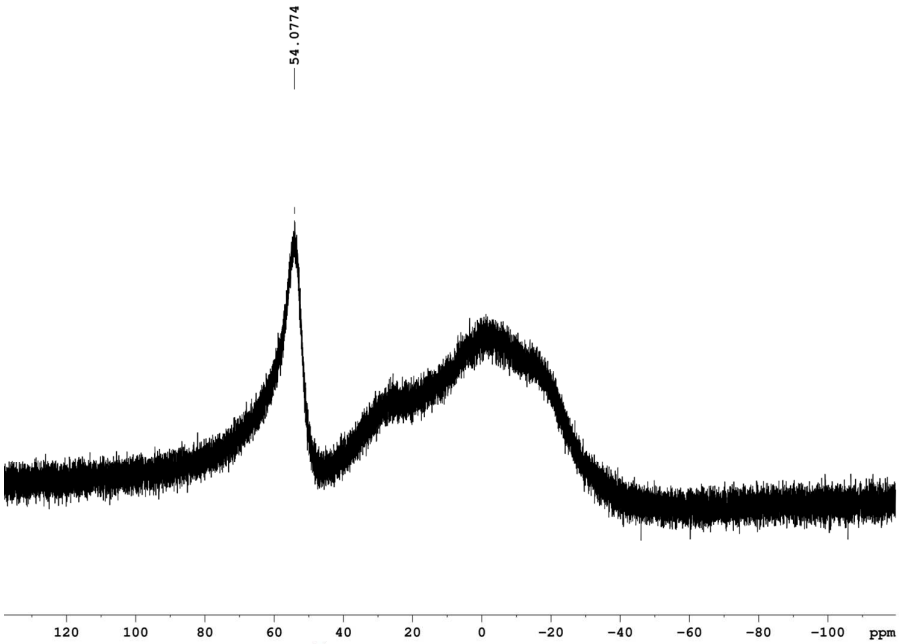

Figure S21: ^{11}B NMR of [**1-Ba**][OTf] in CD_2Cl_2

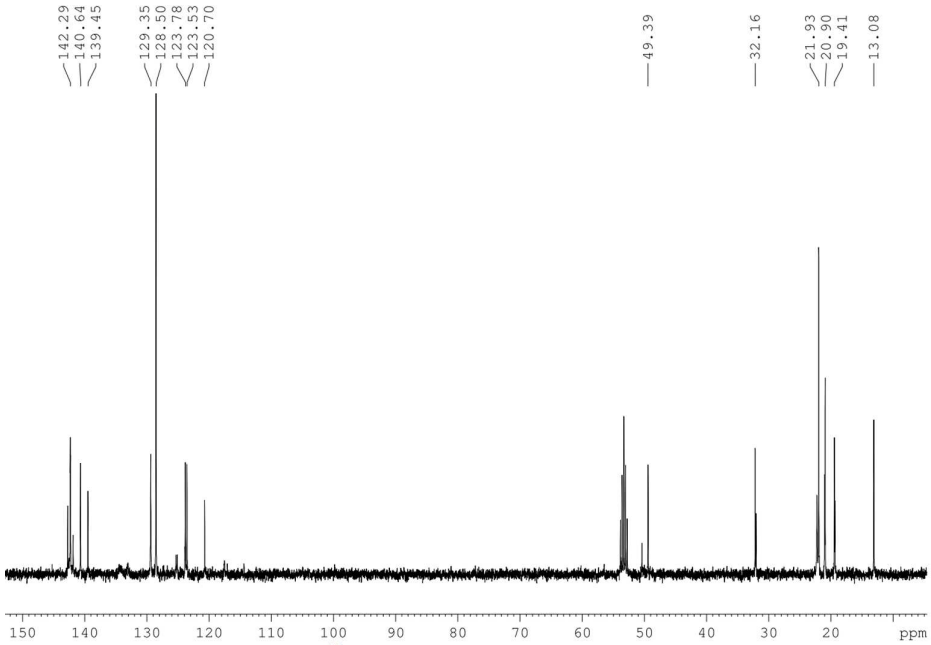

Figure S22: ^{13}C NMR of [**1-Ba**][OTf] in CD_2Cl_2

(5) (3-Aa)

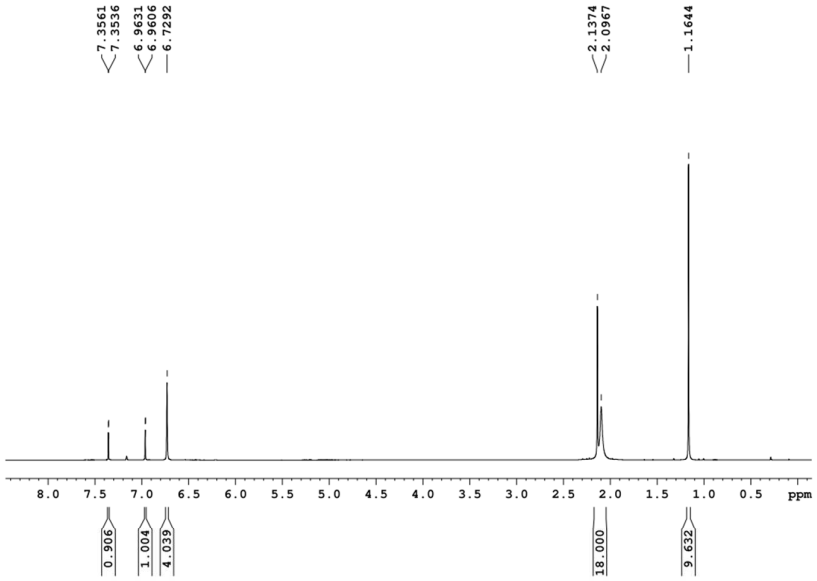

Figure S23: ^{1}H NMR of (**3-Aa**) in C_6D_6

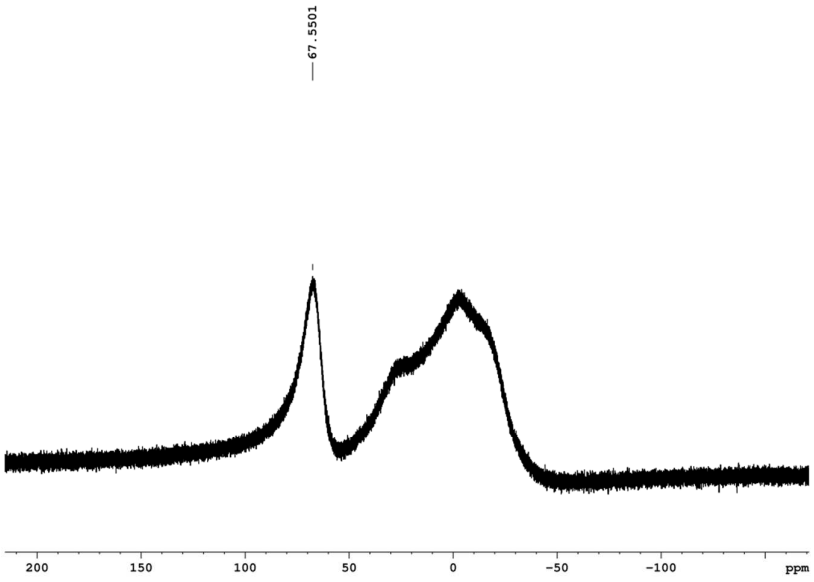

Figure S24: ^{11}B NMR of (**3-Aa**) in C_6D_6

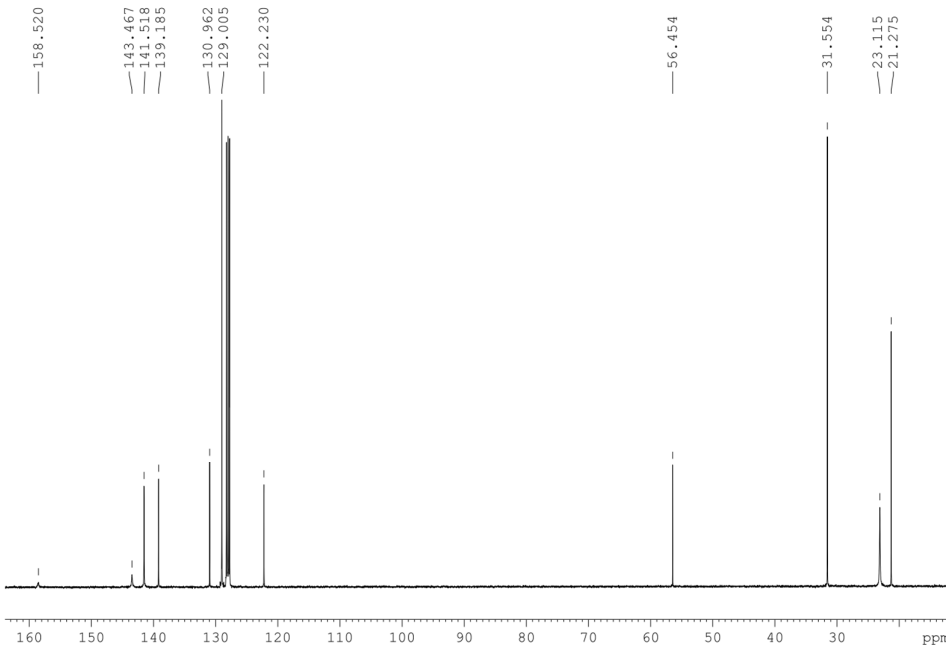

Figure S25: ^{13}C NMR of (**3-Aa**) in C_6D_6

(6) (3-Ab)

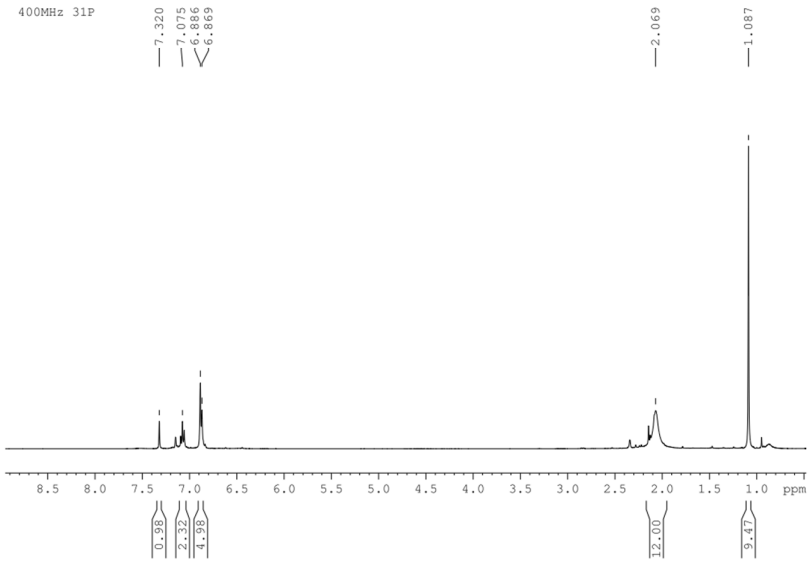

Figure S26: ^{1}H NMR of (**3-Ab**) in C_6D_6

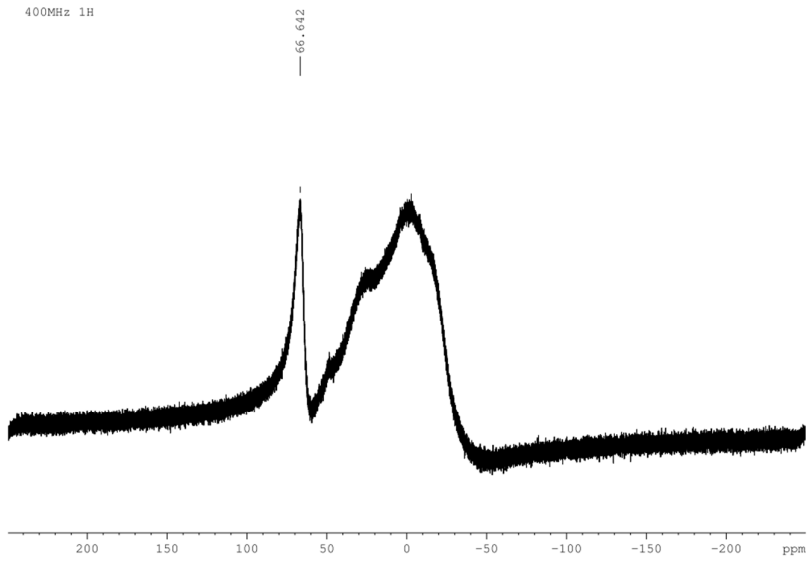

Figure S27: ^{11}B NMR of (**3-Ab**) in C_6D_6

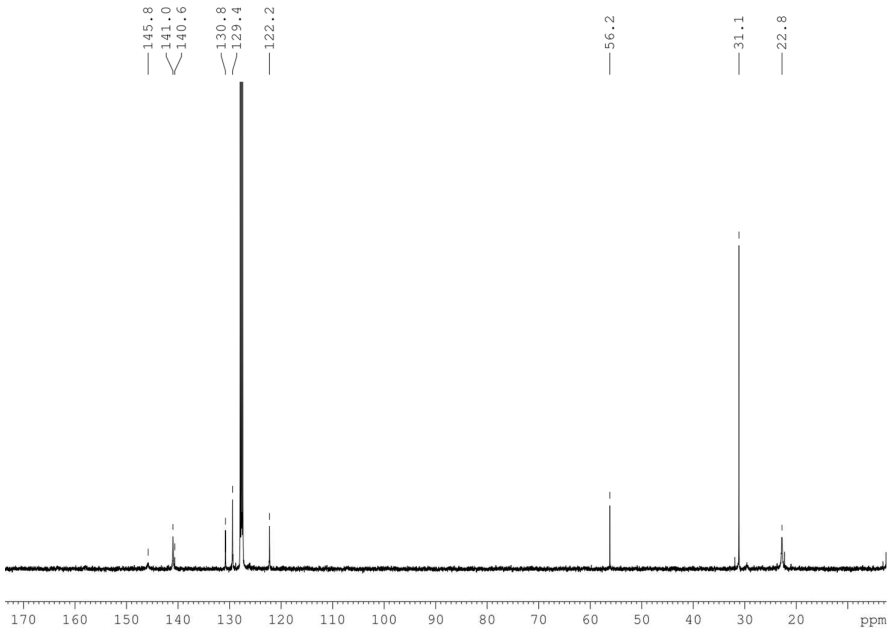

Figure S28: ^{13}C NMR of (**3-Ab**) in C_6D_6

(7) (3-Bb)

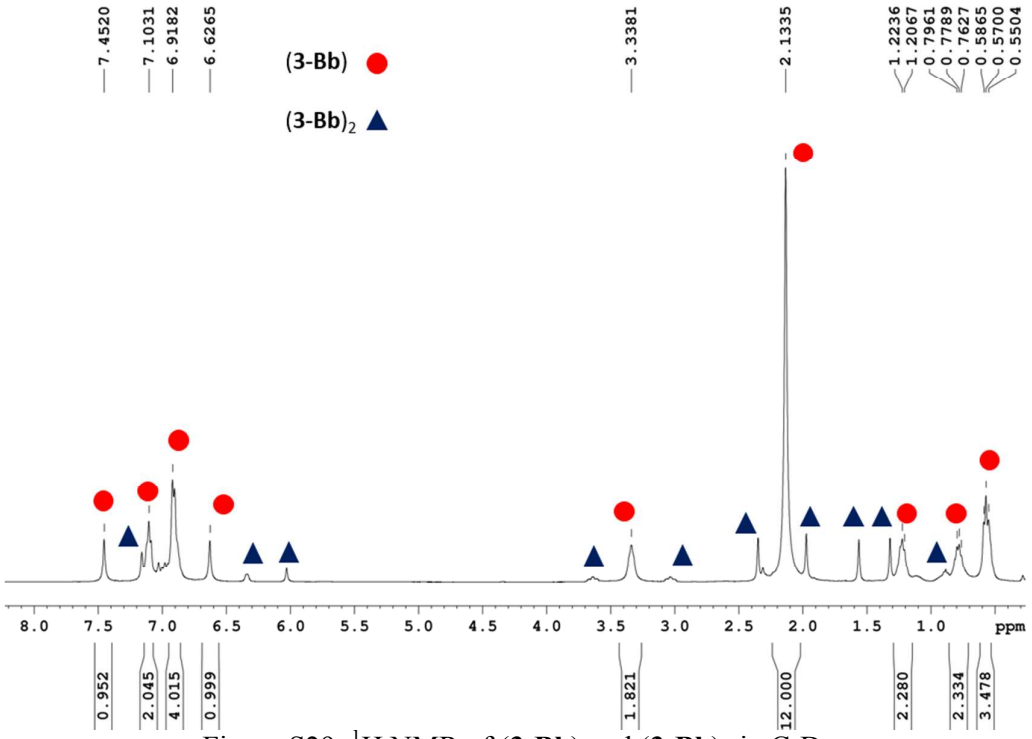

Figure S29: ^{1}H NMR of (**3-Bb**) and (**3-Bb**)$_2$ in C_6D_6

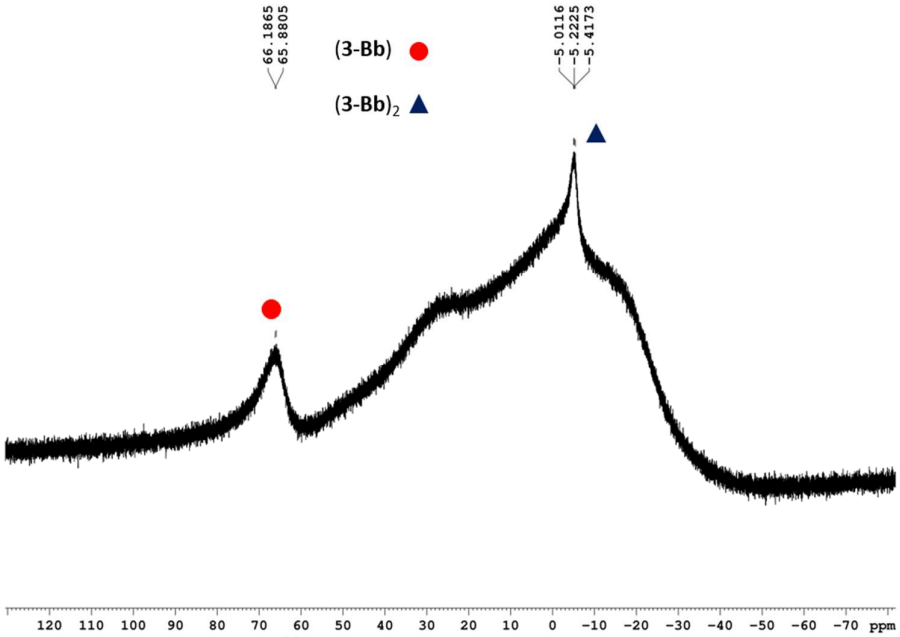

Figure S30: ^{11}B NMR of (**3-Bb**) and (**3-Bb**)$_2$ in C_6D_6

(7) (3-Ba)$_2$

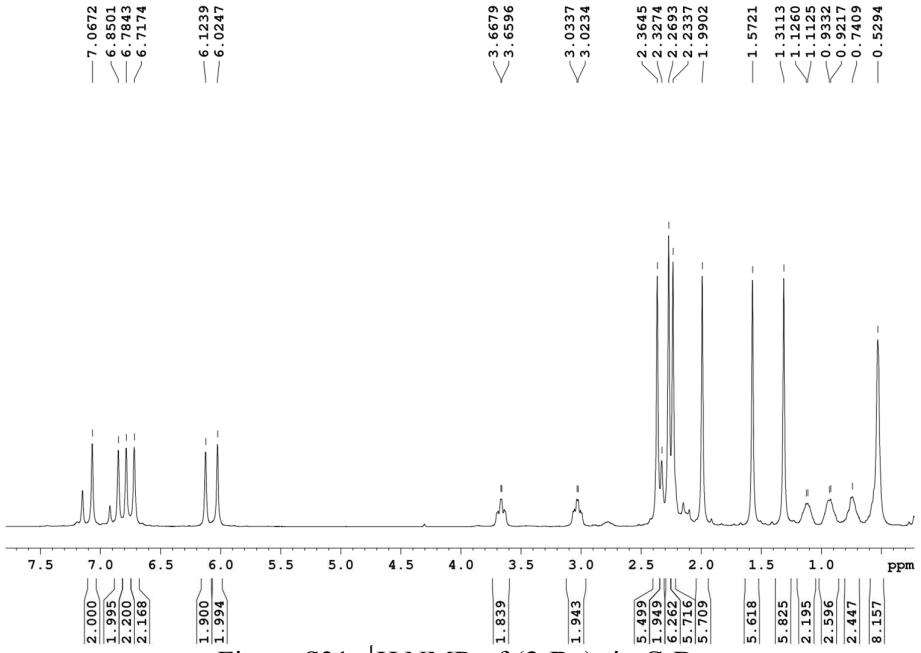

Figure S31: ^{1}H NMR of (**3-Ba**)$_2$ in C_6D_6

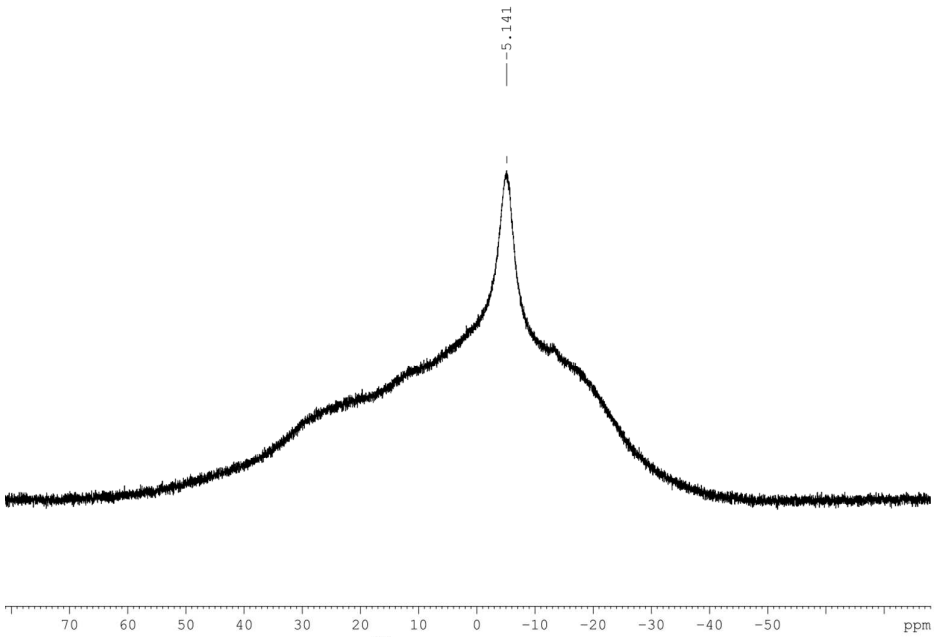

Figure S32: ^{11}B NMR of (**3-Ba**)$_2$ in C_6D_6

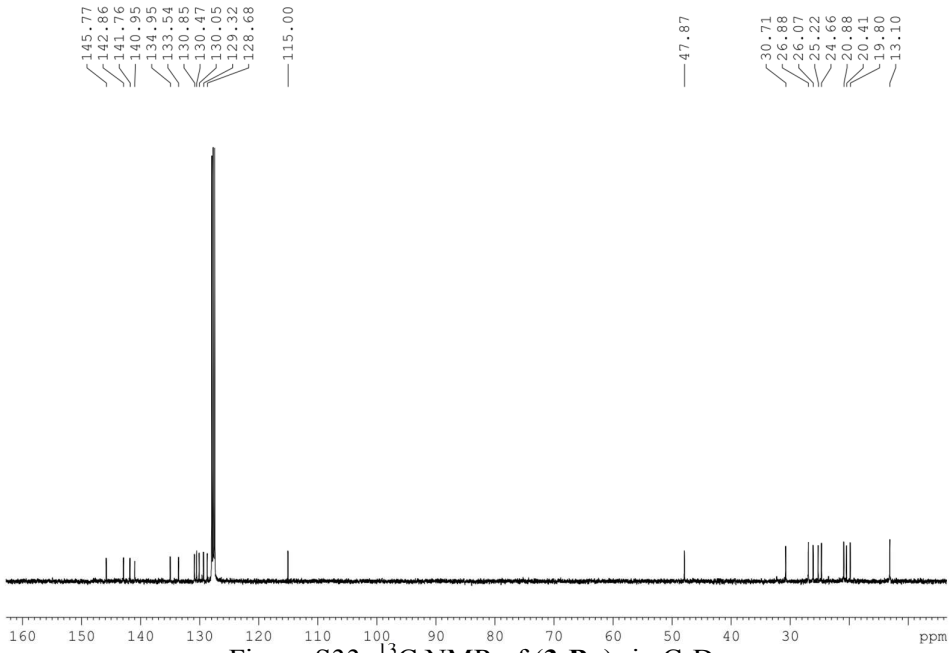

Figure S33: ^{13}C NMR of (**3-Ba**)$_2$ in C_6D_6

(8) (3-Bb)$_2$

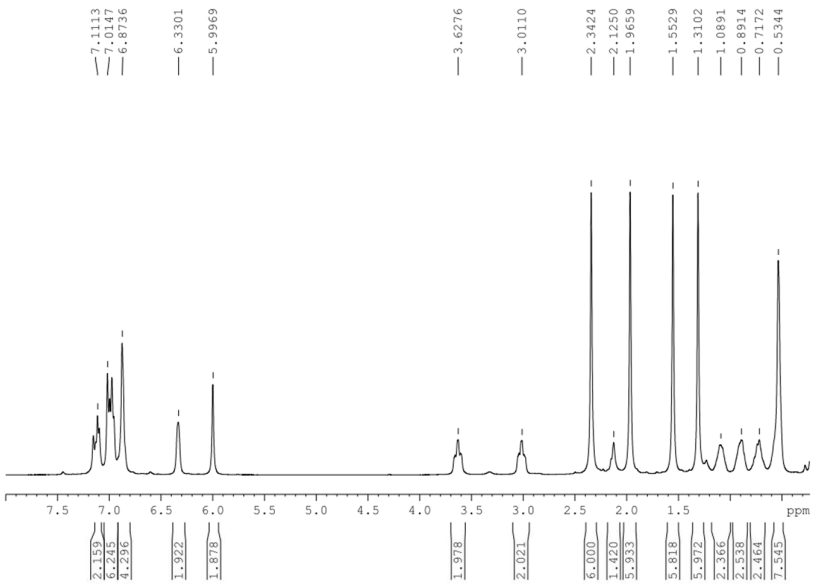

Figure S34: ^{1}H NMR of (**3-Bb**)$_2$ in C_6D_6

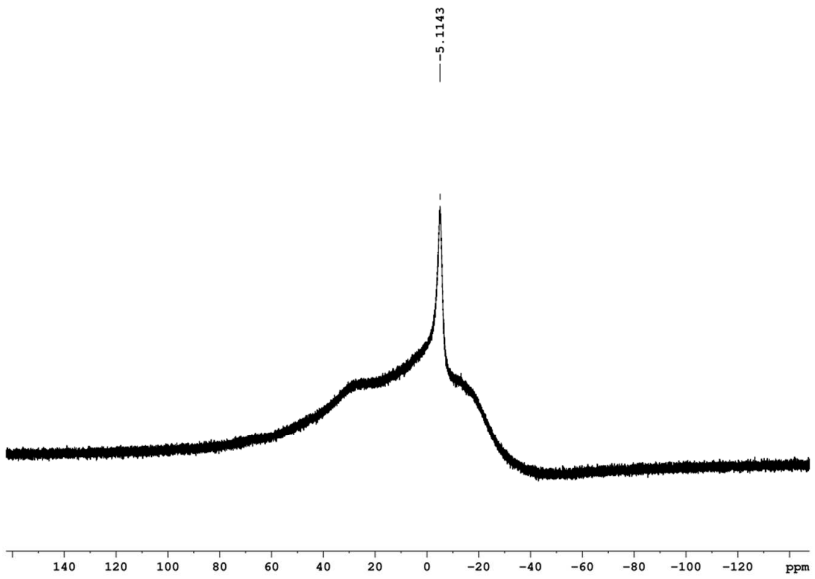

Figure S35: ^{11}B NMR of (**3-Bb**)$_2$ in C_6D_6

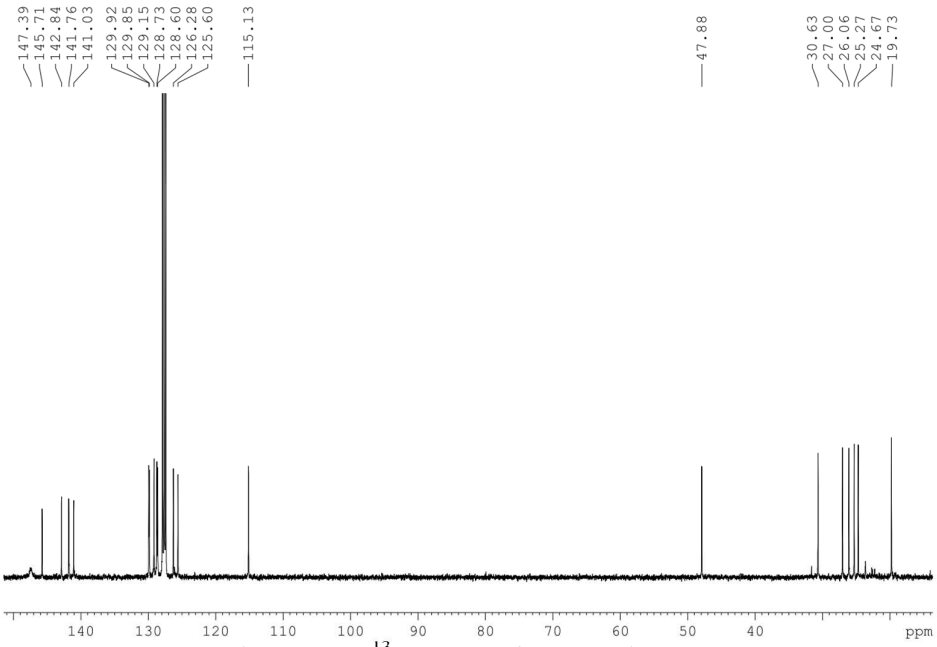

Figure S36: ^{13}C NMR of (**3-Bb**)$_2$ in C_6D_6

5. Theoretical calculations.

(1) Radical 6•

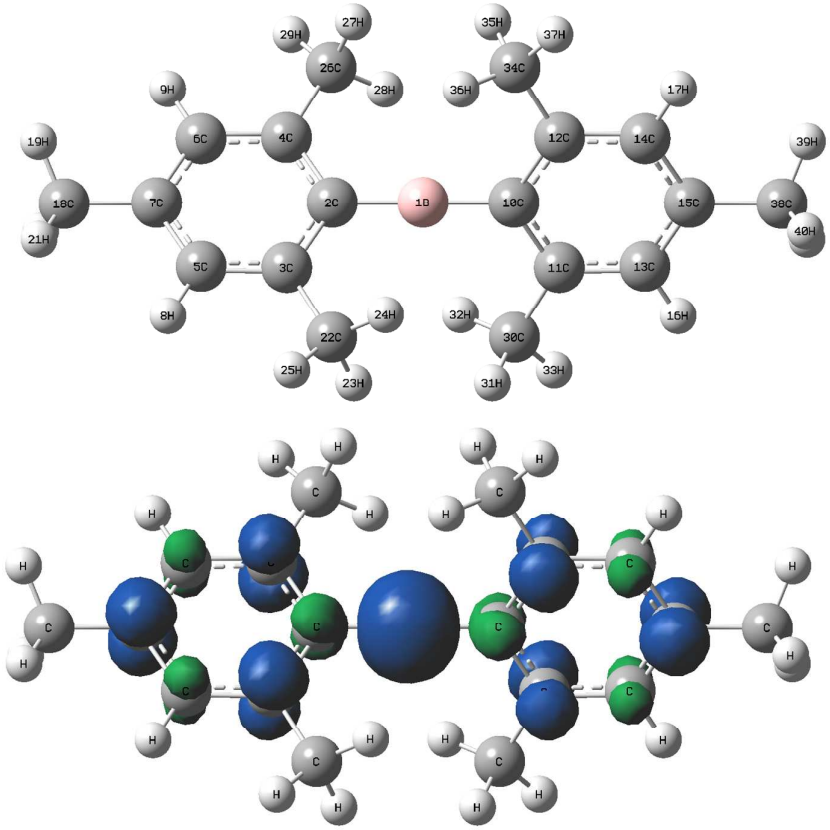

Figure S37: Molecular structure and spin density of 6•(isovalue = 0.004).

(2) Radical 7•

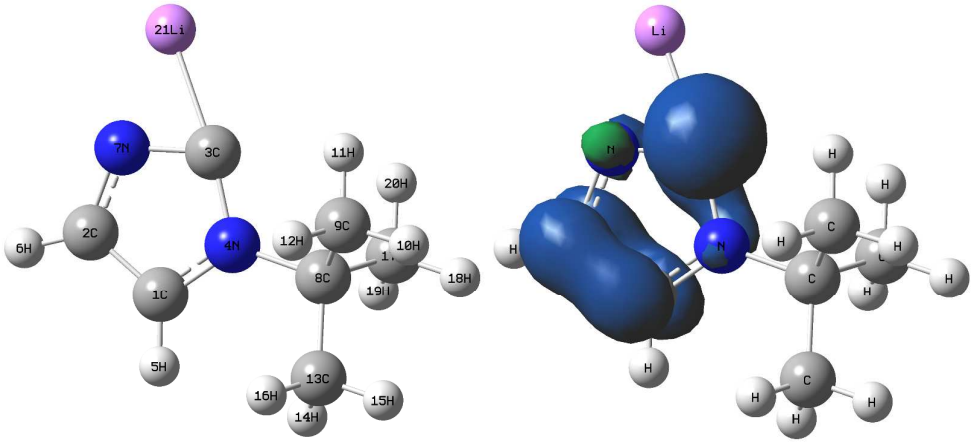

Figure S38: Molecular structure and spin density of 7•(isovalue = 0.002).